

Enhanced transport of two interacting quantum walkers in a one-dimensional quasicrystal with power-law hopping

G. A. Domínguez-Castro and R. Paredes*

Instituto de Física, Universidad Nacional Autónoma de México, Apartado Postal 20-364, México City 01000, Mexico

(Received 19 July 2021; accepted 17 August 2021; published 7 September 2021)

We report a robust delocalization transition of a pair of hard-core bosons moving in a one-dimensional quasicrystal with power-law hopping. We find that in the regime of strong interactions quasiperiodicity first suppresses the transport, as in the usual Anderson picture, and then, transport is enhanced when the quasiperiodic modulation is increased. By introducing an effective Hamiltonian, valid for strong interactions, we unveil the mechanism behind the delocalization transition. Stationary single-particle properties, as well as two-particle correlations, confirm all of our findings. Extensive numerical calculations lead us to establish the values of quasiperiodic modulation, interparticle interactions, and power hops for which the delocalization takes place. Our results are of direct relevance to current experiments of systems with long-range interactions.

DOI: [10.1103/PhysRevA.104.033306](https://doi.org/10.1103/PhysRevA.104.033306)

I. INTRODUCTION

Quantum walks, the quantum counterpart of classical random walks [1], represent optimal platforms for performing efficient quantum algorithms [2,3], exploring topological phases [4], modeling certain photosynthesis processes [5,6], and probing nontrivial dynamics in clean and disordered media in the presence or absence of interactions [7–13]. The wide range of applications that quantum walkers yield has driven its experimental realization in several platforms such as trapped ions [14,15], photons in linear and nonlinear waveguides [16–18], and ultracold atomic gases confined in one-dimensional optical lattices [19–21]. As a matter of fact, due to the high tunability and control that these systems offer, a comprehensive study of a single or many quantum walkers is achievable within the current experimental context.

The dynamics of quantum walkers in disordered media has been widely used for investigating the transport properties of systems belonging to condensed matter [8–10,12,22–24]. As revealed by those studies, the spreading of particles is altered since the disorder breaks the translational symmetry in an otherwise perfectly periodic lattice. For instance, in the one-dimensional Anderson model [25,26], any disorder strength yields the exponential localization of the single-particle eigenstates and consequently the absence of particle diffusion. Another widely used model arises in a one-dimensional quasiperiodic lattice, often called the Aubry-André (AA) model [27–29] (or more precisely, the Aubry-André-Azbel-Harper model), where the quasiperiodicity emerges as a consequence of superimposing two lattices with incommensurate periods [30]. To avoid confusion with the uncorrelated or random disorder, we use interchangeably quasidisorder to indicate the quasiperiodicity introduced in the AA model. In the AA model there is a threshold in the quasidisorder

strength that signals the transition between extended ergodic and localized single-particle eigenstates; therefore, the single-particle diffusion changes from being ballistic, where the spread of the walker grows linearly in time, to becoming null, where the particle is constrained to its initial position [30]. Both the Anderson and the AA models are characterized by being tight-binding schemes where the tunneling beyond nearest neighbors (NN) is exponentially suppressed. This constraint, together with the spatial disorder, reduces the diffusion of the walkers to the two extreme cases: ballistic and null regimes. To enrich the dynamics exhibited by the walkers, one can replace the nearest-neighbor tunneling with a hopping whose amplitude follows a power law. This modification is of particular interest since power-law interactions arise in many important systems, such as trapped ions [14,15], polar molecules [31,32], Rydberg atoms [33,34], nuclear spins in solid-state systems [35], photosynthetic complexes [36,37], and atoms in photonic crystal waveguides [38]. Previous studies of the resulting eigenstates in the AA model have shown that the inclusion of power-law hopping induces the appearance of energy-dependent mobility edges [39,40] and multifractal states [40]. Another relevant result, within the single-particle scheme, is a recent analysis that considers all-to-all hopping and random disorder [41]. Reference [42] revealed a disorder-enhanced transport regime in a one-dimensional nanostructure. For the two-body case, the literature has focused on the NN tunneling [43,44].

The purpose of the present paper is precisely the study of the interplay among quasidisorder, interparticle interactions, and power-law hopping, on the spreading of two hard-core bosons initially localized in the middle of a one-dimensional lattice. In particular, we demonstrate that within the strongly interacting regime, a delocalization transition arises as the quasiperiodic modulation increases. This is in stark contrast to the general knowledge that quasidisorder always results in transport suppression. To explain this unusual behavior, we introduce an effective Hamiltonian that describes the motion

*rosario@fisica.unam.mx

of the walkers as a bound particle whose dynamics is shielded from the power-law hopping. The transport of the composite object is suppressed until the quasidisorder is large enough to close the energy gap between the bound and unbound states. Closing the energy gap allows the walkers to dissociate and delocalize, since unbound states are less prone to show strong localization. Our results are of relevance in correlated two-particle studies [45,46], quantum state transfer protocols of long-range spin systems [47], and quasiparticle propagation experiments in trapped ions [48,49], among other examples. Definitely, two-body transport studies can shed light on more complex phenomena such as the many-body localization of interacting long-range systems [50–53]. In contrast to previous studies of quantum walkers moving in a disordered medium [8–10,12], we demonstrate that the quasidisorder can enhance the transport of the walkers. Additionally, we provide a theoretical model that supports our findings.

The manuscript is organized as follows. In Sec. II we introduce and briefly discuss the model considered to follow the dynamics of the pair of hard-core bosons. Afterwards, in Sec. III, we exhibit the delocalization transition and introduce an effective Hamiltonian that describes the motion of the walkers within the strongly interacting regime. In Sec. IV, we employ the survival probability to characterize the delocalization transition. Finally, in Sec. V, we summarize and conclude the manuscript.

II. MODEL

The Hamiltonian that describes two interacting hard-core bosons moving in a one-dimensional quasicrystal with inter-site couplings decaying as a power law is given by

$$\hat{H} = -J \sum_{i,j \neq i} \frac{1}{|i-j|^\alpha} \hat{b}_i^\dagger \hat{b}_j + \Delta \sum_i \cos(2\pi\beta i + \phi) \hat{n}_i + U \sum_i \hat{n}_i \hat{n}_{i+1}, \quad (1)$$

where \hat{b}_i (\hat{b}_i^\dagger) is the bosonic annihilation (creation) operator at site i , $\hat{n}_i = \hat{b}_i^\dagger \hat{b}_i$ is the corresponding particle number operator, J is the tunneling amplitude between nearest neighbors, and U is the nearest-neighbor interaction amplitude. Quasiperiodicity in the lattice is introduced through the second term in Eq. (1), in which the parameter Δ modulates the strength, $\beta = (\sqrt{5} - 1)/2$ is the incommensurable parameter, and $\phi \in [0, 2\pi)$ accounts for a random phase. The hard-core constraint $(\hat{b}_i^\dagger)^2 = 0$ implies that no double occupancy is allowed. However, the operators \hat{b}_i and \hat{b}_j^\dagger satisfy the usual bosonic commutation relations when $i \neq j$. Here we should point out that the double-occupancy restriction emerges naturally in systems where only one excitation per site is allowed, for instance, Rydberg states in neutral atoms, rotational states in polar molecules, and hyperfine states in trapped ions. Periodic boundary conditions $\hat{n}_{L+1} = \hat{n}_1$, with L being the number of sites in the lattice, shall be considered to numerically solve the model.

Since the aim of this paper is to focus on the two-particle dynamics, we provide in the next lines a succinct collection of statements associated with the interacting and noninteracting

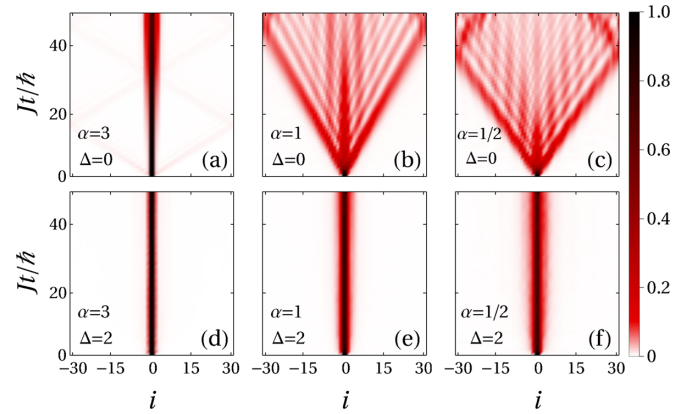


FIG. 1. Time evolution of the density distribution $n_i(t)$ of two walkers initially occupying adjacent sites on the center of the lattice. Quasidisorder and power-law hops are indicated in each panel. The interparticle interaction for all panels is $U/J = 8$.

cases of the Hamiltonian in Eq. (1). While for short-range hopping, $\alpha \gg 1$ and $U/J = 0$, the well-known AA model [27–29] is recovered, for arbitrary values of α the Hamiltonian in Eq. (1) is better known as the generalized-Aubry-André (GAA) model [40]. The AA model exhibits extended ergodic single-particle states for $\Delta/J < 2$, multifractal states for $\Delta/J = 2$, and localized states for $\Delta/J > 2$. Meanwhile, the GAA model displays a plethora of mobility edges that splits extended and localized states for $\alpha \gtrsim 1$ and multifractal single-particle states for long-range hops of $\alpha < 1$ [40]. For the two-body case with NN hopping, it has been shown that the interaction enhances the formation of localized pairs [43]. The effects of including power-law tunneling are not yet explored and it is the aim of this paper to address them.

III. PAIR BREAKING AS A MECHANISM OF DELOCALIZATION

To unveil the effects of interparticle interactions, quasidisorder, and power-law hopping on the two-body transport properties, we consider the quantum walk of a pair of interacting hard-core bosons initially localized at adjacent lattice sites in the middle of a chain having $L = 62$ sites. The time evolution of the initial state $|\psi(t=0)\rangle = \hat{b}_{L/2+1}^\dagger \hat{b}_{L/2}^\dagger |0\rangle$ is calculated by using the eigenstates $|\phi_m\rangle$ and their corresponding eigenenergies E_m obtained from the exact diagonalization of the Hamiltonian in Eq. (1), that is,

$$|\psi(t)\rangle = \sum_m C_m e^{-iE_m t/\hbar} |\phi_m\rangle, \quad (2)$$

where $C_m = \langle \phi_m | \psi(0) \rangle$. To illustrate the most distinctive findings in the two-particle spreading, we chose a set of parameters $(U/J, \Delta/J)$ and three different values of α ($\alpha = 3, 1, \text{ and } 1/2$) for which peculiar transport effects emerge. All the calculations for finite quasidisorder were obtained from the average of 400 random uniformly distributed phases $\phi \in [0, 2\pi)$. In Fig. 1 we show the time evolution of the single-particle density $n_i(t) = \langle \psi(t) | \hat{b}_i^\dagger \hat{b}_i | \psi(t) \rangle$ for both null and finite quasidisorder strength when $U/J = 8$. A striking result shown in Figs. 1(a)–(c) is the clearly visible conelike

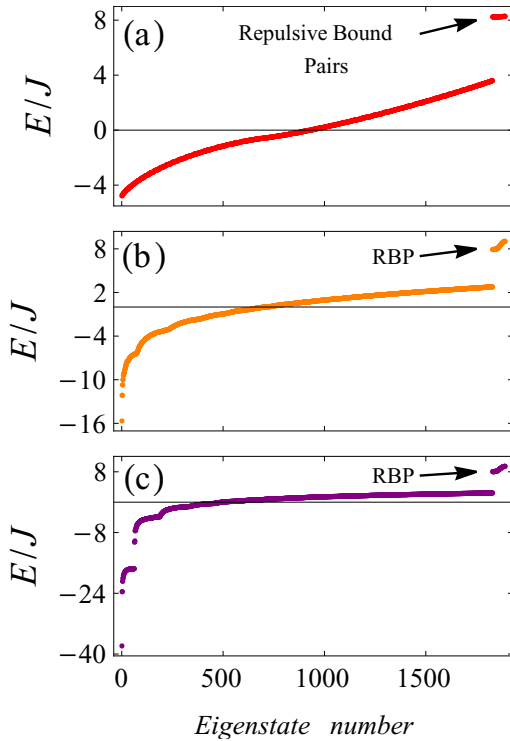


FIG. 2. Energy spectrum of the Hamiltonian in Eq. (1) for $\Delta/J = 0$ and $U/J = 8$. Panels (a), (b), and (c) correspond to power-law hopping values of $\alpha = 3, 1,$ and $1/2$, respectively.

propagation front that appears even in the case of $\alpha = 1/2$. This is a very interesting result that deserves attention, because while such a definite cone emerges in the single quantum walker case for short-range hops [20], in contrast, long-range hops ($\alpha < 1$) do not lead to a sharp cone [54,55]. As we shall see, this behavior must be attributed to both interactions and power-law hopping.

For repulsive interactions ($U/J > 0$), the particles can bind together into a composite object called a repulsive bound pair (RBP), or also termed a bound nearest-neighbor dimer [56–59]. The energy of the repulsive bound pairs is located above the energy of the unbound states [59,60]. As can be seen from Fig. 2, the energy spectrum of the Hamiltonian in Eq. (1) for $\Delta/J = 0$, $U/J = 8$, and $\alpha = 3, 1,$ and $1/2$, has an energy gap that separates unbound and bound states. The black arrow in each panel indicates the location of the high-energy states, that is, the repulsive bound pair states. Given the fact that the energy gap is large enough, the dimer is dynamically stable and therefore unable of dissociating by converting the interaction energy into kinetic energy.

The RBP has the peculiarity of moving around the lattice with both particles in adjacent sites; that is, the walkers propagate as a pair. Consequently, the most relevant Fock states participating in the dynamics of the walkers are those where the particles are in adjacent sites, namely, those Fock states that belong to the subspace $\mathcal{H}_U = \{|n_1 \cdots n_L\rangle \in \mathcal{H} : n_i = n_{i+1} = 1 \forall i \in [1, L]\}$, with \mathcal{H} being the Hilbert space of all Fock states with two hard-core bosons on a lattice with L sites. As a matter of fact, one can quantify the relevance of the states belonging to \mathcal{H}_U on the dynamics of the walkers by

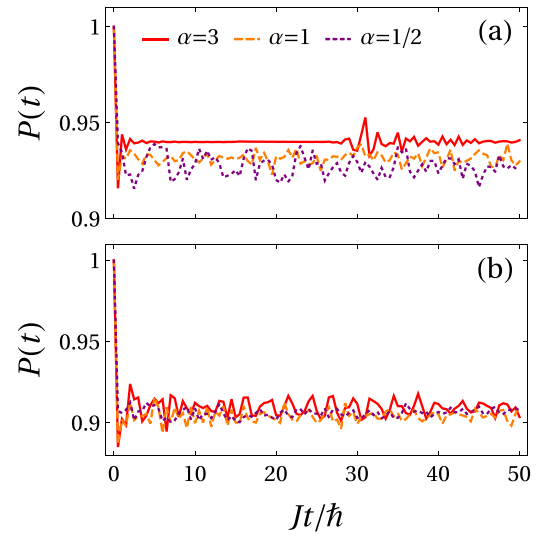


FIG. 3. Time evolution of the expectation value of the projector operator $\hat{P} = \sum_i \hat{n}_i \hat{n}_{i+1}$. Panel (a) corresponds to $\Delta/J = 0$ and $U/J = 8$, whereas panel (b) considers $\Delta/J = 2$ and $U/J = 8$. The values of α are indicated in different colors and line patterns.

considering a projector operator \hat{P} acting on the states of \mathcal{H}_U . The projector operator \hat{P} is defined as follows:

$$\hat{P} = \sum_i \hat{n}_i \hat{n}_{i+1}. \quad (3)$$

In Fig. 3 we show the expectation value of the operator \hat{P} , $P(t) = \langle \psi(t) | \hat{P} | \psi(t) \rangle$, as a function of time. Figures 3(a) and 3(b) correspond to quasidisorder strength $\Delta/J = 0$ and 2 , respectively, both panels are for $U/J = 8$, and the values of α are indicated in colors. Since $P(t)$ takes values close to unity, it is reasonable to state that the dynamics of the walkers can be satisfactorily described by considering only the states belonging to \mathcal{H}_U .

Having established the relevance of the subspace \mathcal{H}_U , one can introduce an effective Hamiltonian H_{eff} acting solely on \mathcal{H}_U . By rewriting \hat{H} in Eq. (1) as $\hat{H} = \hat{H}_0 + \hat{V}$, where

$$\begin{aligned} \hat{H}_0 &= U \sum_i \hat{n}_i \hat{n}_{i+1} = U \hat{P}, \\ \hat{V} &= -J \sum_{i,j \neq i} \frac{1}{|i-j|^\alpha} \hat{b}_i^\dagger \hat{b}_j + \Delta \sum_i \cos(2\pi \beta i + \phi) \hat{n}_i, \end{aligned} \quad (4)$$

and noticing that $\hat{H}_0 |\Psi\rangle = U |\Psi\rangle$ with $|\Psi\rangle \in \mathcal{H}_U$, then up to first order in \hat{V}/U , $\hat{H}_{\text{eff}} = \hat{P}(\hat{H}_0 + \hat{V})\hat{P}$. After straightforward algebra, one can show that

$$\begin{aligned} \hat{H}_{\text{eff}} &= \hat{P} - \frac{J}{2^\alpha U} \sum_i \hat{n}_{i+1} (\hat{b}_i^\dagger \hat{b}_{i+2} + \hat{b}_{i+2}^\dagger \hat{b}_i) \\ &\quad + \frac{2\Delta}{U} \cos(\pi \beta) \sum_i \cos(2\pi \beta i + \phi) \hat{n}_i \hat{n}_{i+1}. \end{aligned} \quad (5)$$

Since \hat{P} plays no role on the dynamics, it can be safely omitted. Thus, in terms of the hard-core bose operators \hat{b}_i^\dagger and \hat{b}_i (see Appendix A), the effective Hamiltonian acquires the

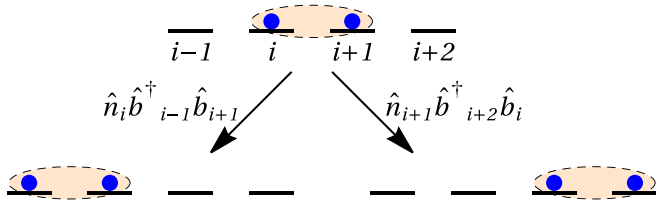


FIG. 4. Schematic representation of the density-dependent next-nearest-neighbor hopping of the pair of walkers.

structure of a Bose-Hubbard-like Hamiltonian with the distinctiveness that the nearest-neighbor hopping is replaced by a density-dependent next-nearest-neighbor tunneling, modulated by the coefficient $J/2^\alpha U$, while the on-site interaction is changed for a site-dependent nearest-neighbor interaction whose amplitude is just the sum of the AA quasiperiodic modulation in adjacent sites, that is, $\cos[2\pi\beta i + \phi] + \cos[2\pi\beta(i+1) + \phi] = 2\cos(\pi\beta)\cos[2\pi\beta i + \varphi]$, with $\varphi = \phi + \pi\beta$ times the factor $2\cos(\pi\beta)\Delta/U$. Interestingly, the motion of the walkers circumvents the power-law tunneling; thus, the power α plays a role in the strength of the density-dependent next-nearest-neighbor hopping $J/2^\alpha U$ only. Notice that as the hopping becomes short-range $\alpha \gg 1$, this contribution vanishes; in fact, this term is completely absent for NN hopping. In contrast to previous studies [43,59,61], the leading contribution to the mobility of the bound pair emerges from the first-order hopping processes $|1_i\rangle|1_{i+1}\rangle \rightarrow |1_{i+2}\rangle|1_{i+1}\rangle$ and $|1_i\rangle|1_{i+1}\rangle \rightarrow |1_i\rangle|1_{i-1}\rangle$ (see the schematic representation of Fig. 4). The effective Hamiltonian in Eq. (5) gives a clear explanation of the conelike propagations shown in Figs. 1(a)–(c) since the walkers behave as a single composite object moving in a lattice without power-law hops.

We now turn to the behavior shown in Figs. 1(d)–(f). When disorder takes nonzero values, the energy gap between bound and unbound states reduces, thus jeopardizing the stability of the pair. However, as shown in Fig. 3(b), the most relevant Fock states involved in the dynamics of the walkers are still those that belong to \mathcal{H}_U when $\Delta/J = 2$ and $U/J = 8$ for the three power-law hops $\alpha = 3, 1,$ and $1/2$. In other words, the dimer endures for $\Delta/J = 2$.

One can suspect that the suppression of transport shown in Figs. 1(d)–(f) is due to the localization of the eigenstates belonging to \hat{H}_{eff} when $\Delta/J = 2$. This can be confirmed by evaluating the inverse participation ratio (IPR) in the Fock basis of the eigenstates that results from diagonalizing the effective Hamiltonian. The IPR of a normalized state $|\phi_m\rangle$ is evaluated as follows:

$$\text{IPR}_m = \sum_{\{n\}} |\langle \{n\} | \phi_m \rangle|^4, \quad (6)$$

where $|\{n\}\rangle$ is a state of the Fock basis. In Figs. 5(a)–(c) we plot the IPR of the eigenstates belonging to both \hat{H} and \hat{H}_{eff} (inset) in their respective Fock basis when $U/J = 8$ and $\Delta/J = 2$ for $\alpha = 3, 1,$ and $1/2$, respectively. From Fig. 5 one can notice that a fraction of the low-energy states of \hat{H} are not localized, while its high-energy states show strong localization. Conversely, all the eigenstates of \hat{H}_{eff} are localized. Since the dimer motion is described by \hat{H}_{eff} , its transport is suppressed, even though the original Hamiltonian \hat{H} has ex-

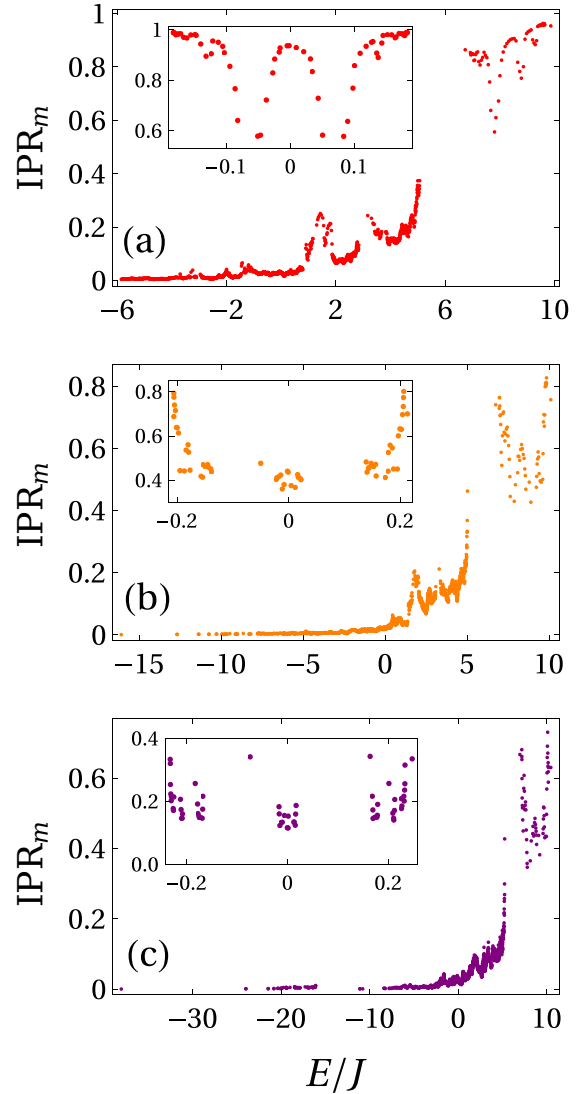


FIG. 5. Inverse participation ratio of the eigenstates belonging to both \hat{H} and \hat{H}_{eff} (inset) for $U/J = 8$ and $\Delta/J = 2$. Panels (a), (b), and (c) correspond to a power-law hopping values of $\alpha = 3, 1,$ and $1/2$, respectively.

tended states. In summary, the dimer still persists for $\Delta/J = 2$ at the price of suppressing its spread.

Another quantity that allows us to recognize the coherent motion of the walkers is the two-particle correlation $\Gamma_{i,j}(t) = \langle \psi(t) | \hat{b}_i^\dagger \hat{b}_j^\dagger \hat{b}_j \hat{b}_i | \psi(t) \rangle$. This two-body correlation function provides meaningful information regarding the effects of the interparticle interaction on the dynamics of quantum walkers [7,9,62]. In Fig. 6 we show $\Gamma_{i,j}(t)$ after a propagation time of $Jt/\hbar = 20$ for the same parameters as before, that is, $(\Delta/J, U/J) = (0, 8)$, $(\Delta/J, U/J) = (2, 8)$, and the three different values of $\alpha = 3, 1,$ and $1/2$. In agreement with the hard-core constraint, the main diagonal of the correlation function vanishes. However, one can notice that the leading contributions emerge from the first diagonal below and above the main diagonal, thus confirming the formation and coherent motion of the pair. In particular, it supports the above statement that for $\Delta/J = 2$, the pair motion is still a suitable

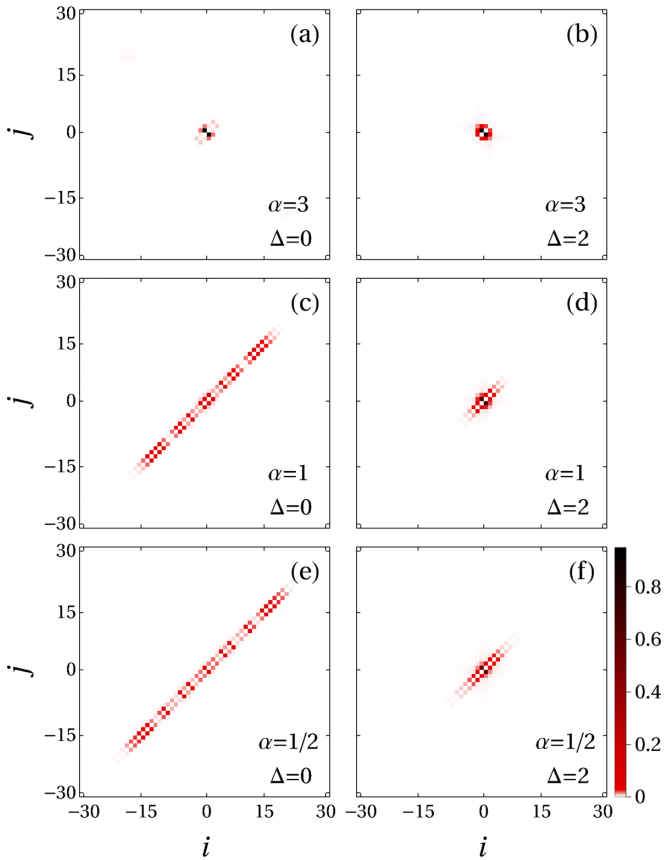


FIG. 6. Two-particle correlation function at $Jt/\hbar = 20$ for two hard-core bosons initially localized at adjacent sites in the middle of a chain. Quasidisorder and power-law hops are indicated in each panel; the interparticle interaction is $U/J = 8$.

picture of the dynamics of the walkers and the only effect of the quasiperiodicity is to suppress the transport.

We want to illustrate now an unforeseen behavior regarding the competence between quasidisorder and interactions. In Fig. 7 we show the time evolution of the single-particle density $n_i(t)$ for $(\Delta/J, U/J) = (4, 8)$ and $(\Delta/J, U/J) = (8, 8)$.

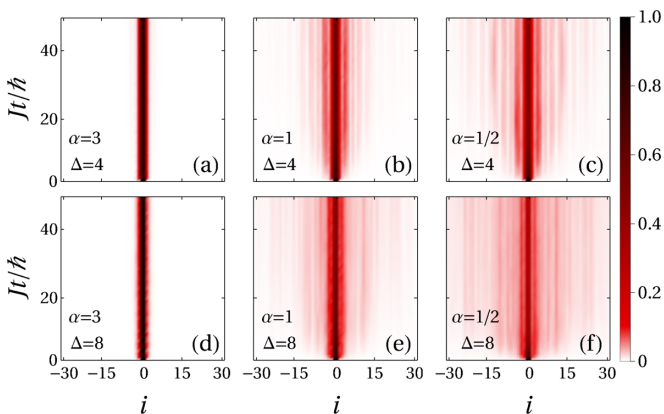


FIG. 7. Time evolution of the single-particle density distribution $n_i(t)$ of two walkers initially occupying adjacent sites on the center of the lattice. Quasidisorder and power-law hops are indicated in each panel. The interparticle interaction for all panels is $U/J = 8$.

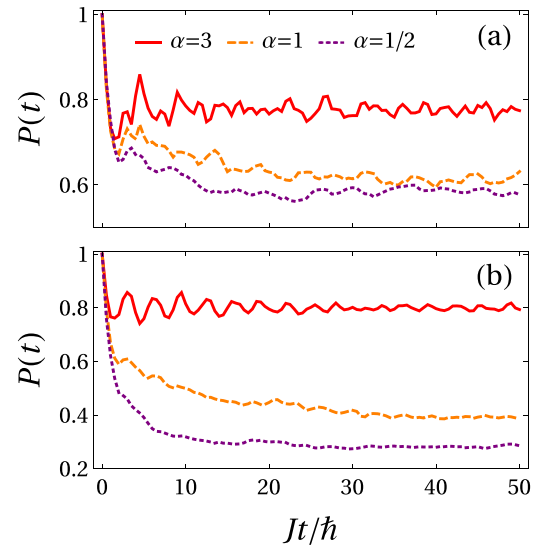


FIG. 8. Time evolution of the expectation value of the projector operator $\hat{P} = \sum_i \hat{n}_i \hat{n}_{i+1}$. Panel (a) corresponds to $(\Delta/J, U/J) = (4, 8)$, whereas panel (b) considers $(\Delta/J, U/J) = (8, 8)$. The power-law hopping values are $\alpha = 3$ (red solid line), $\alpha = 1$ (orange dashed line), and $\alpha = 1/2$ (purple dotted line).

One can notice that, for $\alpha = 3$, Figs. 7(a) and 7(d) display a similar appearance; that is, the diffusion of the walkers is suppressed by interactions and quasiperiodicity. Surprisingly, this is not the case for $\alpha = 1$ and $\alpha = 1/2$, since these profiles achieve expansion to greater distances for $\Delta/J = 4$ and $\Delta/J = 8$ than those for $\Delta/J = 2$ [see Figs. 1(e) and 1(f)], thus contradicting the general notion that the quasidisorder yields suppression of transport.

To understand why the quasiperiodicity restores the transport of the walkers when $\alpha = 1$ and $\alpha = 1/2$, it is instructive to show first that the picture of the walkers moving together breaks down. In Fig. 8(a) we plot the time evolution of $P(t)$ when $\Delta/J = 4$ and $U/J = 8$ for $\alpha = 3, 1$, and $1/2$, whereas Fig. 8(b) considers $\Delta/J = U/J = 8$ for the same values of α . One can notice that now the contribution of the Fock states belonging to \mathcal{H}_U on the dynamics of the walkers is less relevant than the cases exhibited in Fig. 3. In fact this is more evident for $\Delta/J = 8$. Thus, when quasidisorder competes with the interaction, the effective Hamiltonian \hat{H}_{eff} is no longer suitable to describe the spreading of the particles.

To show the effect of quasidisorder on the energy spectrum, in Fig. 9 we plot the eigenenergies of the Hamiltonian in Eq. (1) for $U/J = 8$ and $\Delta/J = 4$ [Figs. 9(a), 9(c), and 9(e)] and for $\Delta/J = U/J = 8$ [Figs. 9(b), 9(d), and 9(f)]. The values of α are the same used throughout the paper. One can notice that for the strengths of quasidisorder considered, the energy gap is now negligible compared to the previous case (see Fig. 2). Consequently, the dynamics of the walkers is no longer exclusively concentrated in the high-energy sector, where dimers states are located, but also in lower-energy states. However, as one can notice from Fig. 10, the low-energy eigenstates have the peculiarity of having an inverse participation ratios lower than those of high-energy states. Therefore, the participation of low-energy states, where the pair is dissociated, enhances the transport of the walkers.

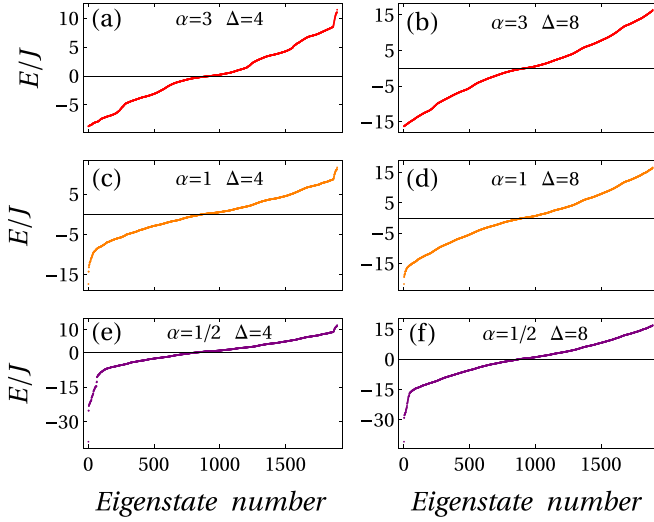


FIG. 9. Energy spectrum of the Hamiltonian in Eq. (1) for $U/J = 8$. Quasisorder strengths and power-law hops are indicated in each panel.

To end this section, in Fig. 11 we show the two-particle correlation function $\Gamma_{i,j}(t)$ after a propagation time of $Jt/\hbar = 20$, for $(\Delta/J, U/J) = (4, 8)$, $(\Delta/J, U/J) = (8, 8)$, and the three different values of $\alpha = 3, 1$, and $1/2$. In contrast with the correlation functions shown in Fig. 6, the diagonals above and below the main diagonal in Fig. 11 are no longer the principal contributions to the correlation functions. Therefore, states where the pair is dissociated contribute the most to the dynamics of the walkers, thus allowing the particles to spread to regions that were not accessible for the case $\Delta/J = 2$.

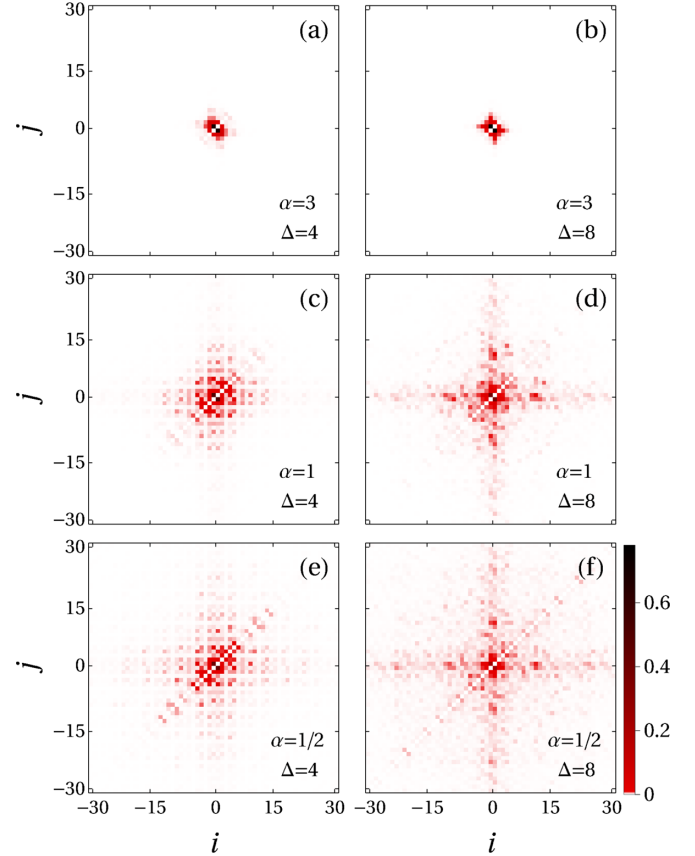


FIG. 11. Two-particle correlation at $Jt/\hbar = 20$ for $U/J = 8$. Quasisorder strengths and power-law hops are indicated in each panel.

IV. SURVIVAL PROBABILITY

Having established the mechanism behind the quasisorder-enhanced transport transition, it is suitable to find a quantity that senses the degree of delocalization of the walkers. For this purpose, we employ the survival probability $f(t)$, which measures the probability of finding the system in its initial state $|\psi(0)\rangle$ at time t ,

$$f(t) = |\langle \psi(0) | \psi(t) \rangle|^2 = |\langle \psi(0) | e^{-i\hat{H}t/\hbar} | \psi(0) \rangle|^2. \quad (7)$$

In terms of the coefficients C_m and the eigenenergies E_m , the survival probability can be written as follows:

$$f(t) = \left| \sum_m |C_m|^2 e^{-iE_m t/\hbar} \right|^2. \quad (8)$$

Previous studies for disordered systems [63,64] have shown that the survival probability provides meaningful information regarding the dynamics of both noninteracting [65] and interacting systems [66,67]. In Figs. 12(a)–(c) we plot the time evolution of the survival probability $f(t)$ for $U/J = 8$ and $\alpha = 3, 1$, and $1/2$, respectively. In general, the time evolution of $f(t)$ shows a decay from its initial value followed by oscillations around an asymptotic value. For long times in the quasisorder-free case, the survival probability oscillates around the value $1/L$ independently of the power-law hop α , and this indicates that the walkers can spread over

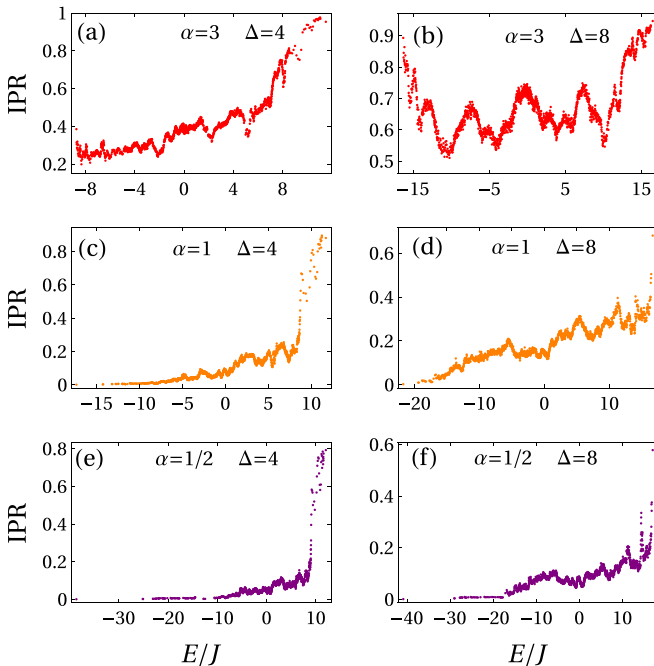


FIG. 10. Inverse participation ratio associated with the eigenstates of the Hamiltonian in Eq. (1) for $U/J = 8$. Quasisorder strengths and power-law hops are indicated in each panel.

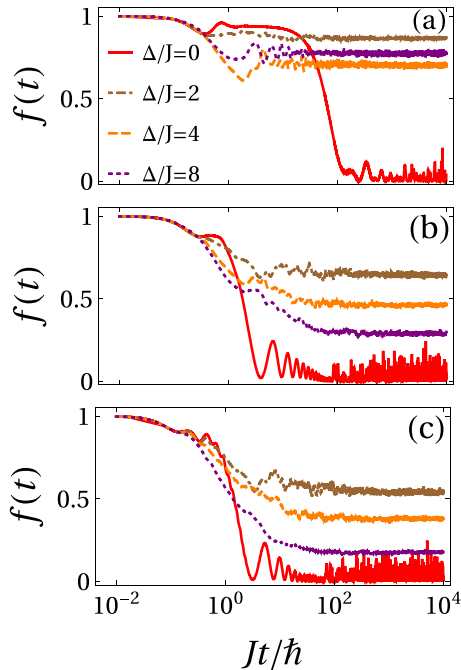


FIG. 12. Survival probability $f(t)$ for $U/J = 8$. Panels (a), (b), and (c) correspond to power-law hopping values of $\alpha = 3$, 1, and $1/2$, respectively. Quasidisorder strengths are $\Delta/J = 0$ (red solid line), $\Delta/J = 2$ (brown dash-dotted line), $\Delta/J = 4$ (orange dashed line), and $\Delta/J = 8$ (purple dotted line).

the whole lattice. For a small quasidisorder strength $\Delta/J = 2$, the asymptotic value of $f(t)$ increases regardless of the value of α . That is, for all cases, suppression of transport is observed, as in the usual Anderson transition. Surprisingly, when quasidisorder increases $\Delta/J = 4$, the asymptotic value of $f(t)$ decreases, indicating the delocalization mentioned in the previous section. Even for $\alpha = 3$, a delocalization is observed. However, the survival probability takes values close to unity, which makes it difficult to observe the delocalization in the density profiles of Fig. 7. Counterintuitively, increasing even more the quasiperiodicity strength leads, in the long-time limit, to a lower value of the survival probability for $\alpha = 1$ and $\alpha = 1/2$; thus, transport is enhanced by quasidisorder. Notice that this is not the case when $\alpha = 3$ since for $\Delta/J = 8$ the survival probability increases as expected.

To smooth the fluctuations in the time evolution of $f(t)$, it is convenient to employ the time average of the survival probability,

$$F(t) = \frac{1}{t} \int_0^t dt' f(t'). \quad (9)$$

In the long-time limit, $F(t)$ saturates to the asymptotic survival probability (ASP) [64]. The saturation point is given by the simple expression

$$F(t \rightarrow \infty) = \sum_m |C_m|^4 = \text{IPR}^{(0)}. \quad (10)$$

To avoid confusion, we point out that $\text{IPR}^{(0)}$ is the inverse participation ratio of the initial state $|\psi(0)\rangle$ in terms of the eigenbasis $|\phi_m\rangle$ of the Hamiltonian in Eq. (1). On the contrary, the quantity IPR_m , used in the previous section, is the inverse

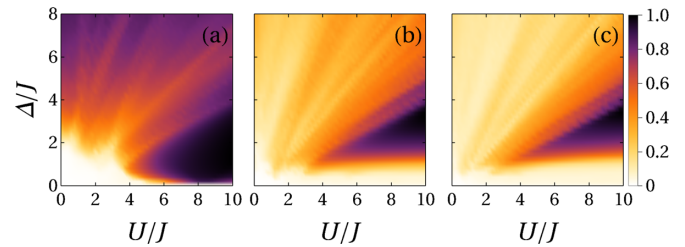


FIG. 13. Asymptotic survival probability $F(t \rightarrow \infty)$ as a function of Δ/J and U/J . Panels (a), (b), and (c) correspond to power-law hopping values of $\alpha = 3$, 1, and $1/2$, respectively.

participation ratio of the eigenstates in terms of the Fock basis. Notice that Eq. (10) links a dynamical quantity with the inherent structure of the eigenstates of the system under investigation.

To establish the values of the quasiperiodic modulation and the interaction between particles for which delocalization occurs, in Figs. 13(a) and 13(b) we condense in a density color scheme the full information of the ASP associated with the competition of quasidisorder vs interactions for $\alpha = 3$, 1, and $1/2$, respectively. From Fig. 13, one can notice two main characteristics. The first one is that, for values of interaction strength $U/J > 4$, the walkers with $\alpha = 3$ get localized for small quasidisorder amplitudes, while the diffusion of walkers with $\alpha = 1$ and $1/2$ is more robust as they localize for larger quasidisorder amplitudes. The second one is that, since interactions yield robustness to the dimer, the delocalization of the pair requires larger quasidisorder amplitudes as the interaction strength increases.

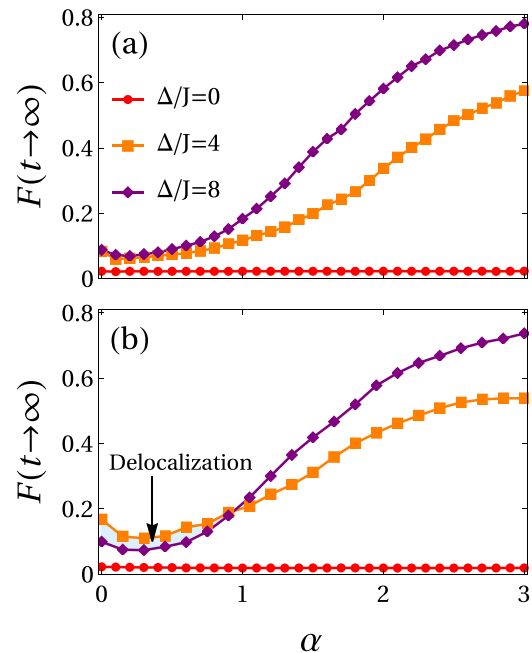


FIG. 14. Asymptotic survival probability $F(t \rightarrow \infty)$ as a function of the power-law hop α for quasidisorder strengths $\Delta/J = 0$ (red circles), $\Delta/J = 4$ (orange squares), and $\Delta/J = 8$ (purple diamonds). Panels (a) and (b) correspond to an interparticle interaction of $U/J = 1$ and $U/J = 4$, respectively.

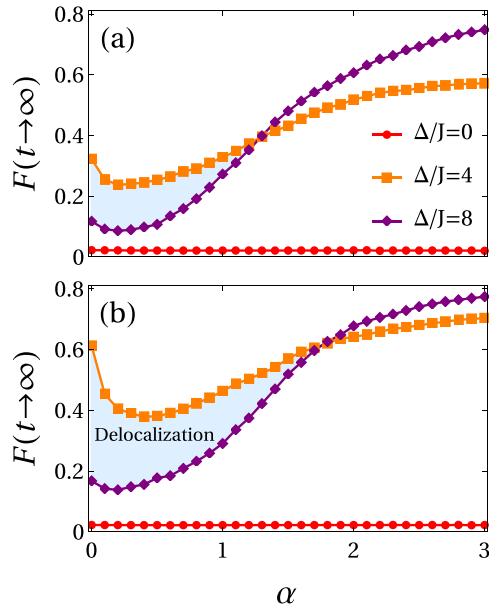


FIG. 15. Asymptotic survival probability $F(t \rightarrow \infty)$ as a function of the power-law hop α for quasidisorder strengths $\Delta/J = 0$ (red circles), $\Delta/J = 4$ (orange squares), and $\Delta/J = 8$ (purple diamonds). Panels (a) and (b) correspond to interparticle interactions of $U/J = 6$ and $U/J = 8$, respectively.

To conclude this section, we unveil the role of the power-law hop in the delocalization transition. For this purpose, in Figs. 14(a) and 14(b) we evaluate the ASP as a function of α for several quasidisorder strengths and interparticle interactions $U/J = 1$ and $U/J = 4$, respectively. For the smallest interaction strength $U/J = 1$, the ASP increases with the quasidisorder as in the usual Anderson scheme. However, this is not the case for $U/J = 4$ since there is a value of α for which the ASP decreases with an increase in the quasiperiodicity. The blue region bounded by the curves $\Delta/J = 4$ and $\Delta/J = 8$ indicates the space of parameters for which the quantum walkers delocalize and, therefore, perform transport assisted by quasidisorder. In Figs. 15(a) and 15(b), we show the ASP as a function of α for interaction magnitudes of $U/J = 6$ and $U/J = 8$, respectively. Figures 14 and 15 reveal that, as the interaction between the walkers increases, the delocalization region enlarges. Interestingly, as shown in Fig. 15(b), the delocalization transition can take place for short ($\alpha > 1$) and long ($\alpha < 1$) tunneling ranges. In contrast to the recently disorder-enhanced transport transition found in a single-particle model with all-to-all hopping [42], here we unveil the role of a power-law hopping on an interacting two-body delocalization transition.

V. CONCLUSIONS

We have investigated the dynamics of a pair of interacting hard-core bosons moving in a one-dimensional quasicrystal with power-law tunneling $1/r^\alpha$. In particular, by analyzing the time evolution of the one-particle density, the survival probability, and the two-particle correlation function, we have found that, for strong interparticle interactions, transport is suppressed for moderate values of the quasidisorder at first, but then is enhanced as it increases. This result is

in stark contrast with the general notion that quasidisorder always favors localization. To reveal the physics behind the quasidisorder-enhanced transport transition, we introduced an effective Hamiltonian that satisfactorily describes the dynamics of the walkers when the interparticle interaction is the largest energy scale. In this effective Hamiltonian, the walkers move as a composite object whose dynamics is completely shielded from the power-law tunneling. As a result, the dimer gets localized for moderate quasidisorder strengths, as in the usual Anderson picture. However, when the quasiperiodicity competes with the interaction, the stability of the pair is jeopardized and the delocalization emerges as a result of the pair dissociation for certain tunneling ranges.

Using the asymptotic value of the survival probability, we established the regions of parameters in which the delocalization of the walkers takes place. In particular, we first fix the power-law hop and explore the delocalization in diagrams for the strength of the incommensurate potential and the interparticle interaction. To this end, we evaluate the role of the power-law hop for fixed quasidisorder strengths and interactions. Our two-body study brings to light the relevance of dimer formation on the transport properties of disordered systems with power-law hopping. As demonstrated, counterintuitive results regarding the spreading of walkers can emerge when dimer formation is taken into account.

The conclusions here achieved are of primary relevance to more complex phenomena involving many-body systems, in particular, within the experimental context, where the possibility of setting states prepared with pairs can lead to unexpected diffusion regimes. We hope that our work will trigger further theoretical analysis such as, for instance, the determination of the fractal nature of the two-body states in intermediate and long-range hops by means of projected Green's function methods [46], the fate of the quasidisorder-enhanced transport transition within the many-body regime, and the role of dimensionality on transport properties, among others. Our results could be of interest for experiments with trapped ions, Rydberg atoms, and photons in crystal waveguides where exotic transport phenomena with long-range interactions are explored.

ACKNOWLEDGMENTS

This work was partially funded by Grant No. IN108620 from DGAPA (UNAM). G.A.D.-C. acknowledges a CONACYT scholarship.

APPENDIX: EFFECTIVE HAMILTONIAN

In Sec. III we introduced an effective Hamiltonian to describe the dynamics of the pair of walkers within the strongly interacting regime. To show that the quasiperiodic modulation induces a nearest-neighbor interaction between particles, we wrote \hat{H}_{eff} in terms of the creation and annihilation operators of the hard-core bosons. However, it is instructive to define the operators $\hat{a}_i = \hat{b}_i \hat{b}_{i+1}$ and $\hat{a}_i^\dagger = \hat{b}_i^\dagger \hat{b}_{i+1}^\dagger$, which annihilate and create a bound nearest-neighbor dimer located at sites i and $i + 1$. These operators inherit the hard-core constraint of the original bosons, that is, $(\hat{a}_i)^2 = (\hat{a}_i^\dagger)^2 = 0$, but also acquire the nearest-neighbor constraint $\hat{a}_i \hat{a}_{i\pm 1} = \hat{a}_i^\dagger \hat{a}_{i\pm 1}^\dagger = 0$. Addi-

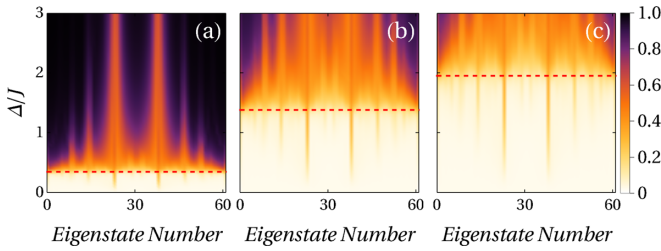


FIG. 16. Inverse participation ratio of all eigenstates of the Hamiltonian in Eq. (A1) as a function of the quasiperiodic modulation. Panels (a), (b), and (c) correspond to power-hopping values of $\alpha = 3, 1,$ and $1/2,$ respectively. The red dashed line corresponds to the critical quasidisorder in Eq. (A2).

tionally, within the subspace \mathcal{H}_U , \hat{a}_i and \hat{a}_i^\dagger obey the standard bosonic commutation relations $[\hat{a}_i, \hat{a}_j^\dagger] = \delta_{ij}$ and $[\hat{a}_i^\dagger, \hat{a}_j^\dagger] = [\hat{a}_i, \hat{a}_j] = 0$, provided $j \neq \{i, i \pm 1\}$. In terms of the dimer operators, the effective Hamiltonian can be written as follows:

$$\hat{H}_{\text{eff}} = -\frac{J}{2^\alpha U} \sum_i (\hat{a}_i^\dagger \hat{a}_{i+1} + \hat{a}_{i+1}^\dagger \hat{a}_i) + \frac{2\Delta}{U} \cos(\pi\beta) \sum_i \cos(2\pi\beta i + \varphi) \hat{a}_i^\dagger \hat{a}_i. \quad (\text{A1})$$

The above Hamiltonian is nothing more than the well-known Aubry-André model with the distinction that the effective tunneling strength is $J' \rightarrow J/(2^\alpha U)$ and the quasiperiodic modulation is $\Delta' \rightarrow 2 \cos(\pi\beta)\Delta/U$. The transition from extended to localized states takes place at $|\Delta'_c/J'| = 2$, which

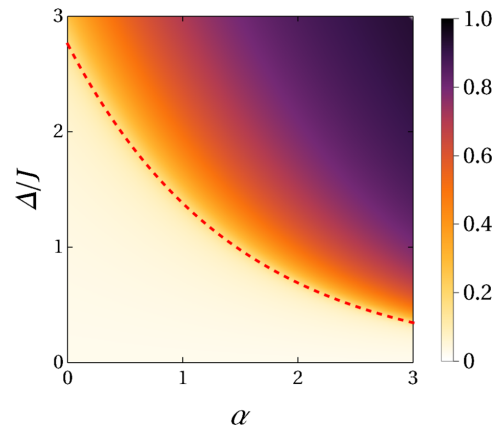


FIG. 17. Average inverse participation ratio as a function of the power-law hop α and the quasidisorder amplitude Δ/J . The red dashed line corresponds to the critical quasidisorder in Eq. (A2).

yields

$$\frac{\Delta_c}{J} = \frac{1}{2^\alpha |\cos(\pi\beta)|}. \quad (\text{A2})$$

In Figs. 16(a)–(c), we show the IPR_m of the eigenstates of the Hamiltonian in Eq. (A1) as a function of the quasidisorder for $\alpha = 3, 1,$ and $1/2,$ respectively. The horizontal dashed red line corresponds to the critical quasidisorder in Eq. (A2).

To explore the average nature of the eigenstates on the α - Δ/J plane, it is convenient to employ the average inverse participation ratio $\overline{\text{IPR}} = \frac{1}{L} \sum_m \text{IPR}_m$. In Fig. 17 we illustrate the $\overline{\text{IPR}}$, and as in the previous figure, the dashed red line corresponds to the critical quasidisorder in Eq. (A2).

-
- [1] Y. Aharonov, L. Davidovich, and N. Zagury, *Phys. Rev. A* **48**, 1687 (1993).
- [2] E. Farhi and S. Gutmann, *Phys. Rev. A* **58**, 915 (1998).
- [3] N. Shenvi, J. Kempe, and K. Birgitta Whaley, *Phys. Rev. A* **67**, 052307 (2003).
- [4] T. Kitagawa, M. S. Rudner, E. Berg, and E. Demler, *Phys. Rev. A* **82**, 033429 (2010).
- [5] R. J. Sension, *Nature (London)* **446**, 740 (2007).
- [6] M. Mohseni, P. Rebentrost, S. Lloyd, and A. Aspuru-Guzik, *J. Chem. Phys.* **129**, 174106 (2008).
- [7] Y. Lahini, M. Verbin, S. D. Huber, Y. Bromberg, R. Pugatch, and Y. Silberberg, *Phys. Rev. A* **86**, 011603(R) (2012).
- [8] D. Wiater, T. Sowiński, and J. Zakrzewski, *Phys. Rev. A* **96**, 043629 (2017).
- [9] T. Chattaraj and R. V. Krems, *Phys. Rev. A* **94**, 023601 (2016).
- [10] L. Wang, N. Liu, S. Chen, and Y. Zhang, *Phys. Rev. A* **95**, 013619 (2017).
- [11] L. Wang, L. Wang, and Y. Zhang, *Phys. Rev. A* **90**, 063618 (2014).
- [12] Y. Lahini, Y. Bromberg, D. N. Christodoulides, and Y. Silberberg, *Phys. Rev. Lett.* **105**, 163905 (2010).
- [13] I. Siloi, C. Benedetti, E. Piccinini, J. Piilo, S. Maniscalco, M. G. A. Paris, and P. Bordone, *Phys. Rev. A* **95**, 022106 (2017).
- [14] F. Zähringer, G. Kirchmair, R. Gerritsma, E. Solano, R. Blatt, and C. F. Roos, *Phys. Rev. Lett.* **104**, 100503 (2010).
- [15] H. Schmitz, R. Matjeschk, Ch. Schneider, J. Glueckert, M. Enderlein, T. Huber, and T. Schaetz, *Phys. Rev. Lett.* **103**, 090504 (2009).
- [16] L. Sansoni, F. Sciarrino, G. Vallone, P. Mataloni, A. Crespi, R. Ramponi, and R. Osellame, *Phys. Rev. Lett.* **108**, 010502 (2012).
- [17] A. S. Solntsev, A. A. Sukhorukov, D. N. Neshev, and Y. S. Kivshar, *Phys. Rev. Lett.* **108**, 023601 (2012).
- [18] M. A. Broome, A. Fedrizzi, B. P. Lanyon, I. Kassal, A. Aspuru-Guzik, and A. G. White, *Phys. Rev. Lett.* **104**, 153602 (2010).
- [19] M. Karski, L. Förster, J.-M. Choi, A. Steffen, W. Alt, D. Meschede, and A. Widera, *Science* **325**, 174 (2009).
- [20] P. M. Preiss, R. Ma, M. E. Tai, A. Lukin, M. Rispoli, P. Zupancic, Y. Lahini, R. Islam, and M. Greiner, *Science* **347**, 1229 (2015).
- [21] T. Fukuhara, P. Schauß, M. Endres, S. Hild, M. Cheneau, I. Bloch, and C. Gross, *Nature (London)* **502**, 76 (2013).
- [22] G. Roati, C. D’Errico, L. Fallani, M. Fattori, C. Fort, M. Zaccanti, G. Modugno, M. Modugno, and M. Inguscio, *Nature (London)* **453**, 895 (2008).
- [23] J. Ghosh, *Phys. Rev. A* **89**, 022309 (2014).
- [24] S. Derevyanko, *Sci. Rep.* **8**, 1795 (2018).

- [25] P. W. Anderson, *Phys. Rev.* **109**, 1492 (1958).
- [26] F. Evers and A. D. Mirlin, *Rev. Mod. Phys.* **80**, 1355 (2008).
- [27] S. Aubry and G. André, *Ann. Israel Phys. Soc.* **3**, 133 (1980).
- [28] P. G. Harper, *Proc. Phys. Soc. A* **68**, 874 (1955).
- [29] M. Ya. Azbel, *Phys. Rev. Lett.* **43**, 1954 (1979).
- [30] G. A. Domínguez-Castro and R. Paredes, *Eur. J. Phys.* **40**, 045403 (2019).
- [31] B. Yan, S. A. Moses, B. Gadway, J. P. Covey, K. R. A. Hazzard, A. M. Rey, D. S. Jin, and J. Ye, *Nature (London)* **501**, 521 (2013).
- [32] L. De Marco, G. Valtolina, K. Matsuda, W. G. Tobias, J. P. Covey, and J. Ye, *Science* **363**, 853 (2019).
- [33] A. Browaeys and T. Lahaye, *Nat. Phys.* **16**, 132 (2020).
- [34] Y. Chougale, J. Talukdar, T. Ramos, and R. Nath, *Phys. Rev. A* **102**, 022816 (2020).
- [35] G. A. Álvarez, D. Suter, and R. Kaiser, *Science* **349**, 846 (2015).
- [36] Y.-C. Cheng and G. R. Fleming, *Annu. Rev. Phys. Chem.* **60**, 241 (2009).
- [37] A. F. Fidler, V. P. Singh, P. D. Long, P. D. Dahlberg, and G. S. Engel, *Nat. Commun.* **5**, 3286 (2014).
- [38] C.-L. Hung, A. González-Tudela, J. I. Cirac, and H. J. Kimble, *Proc. Natl. Acad. Sci. USA* **113**, E4946 (2016).
- [39] D. J. Boers, B. Goedeke, D. Hinrichs, and M. Holthaus, *Phys. Rev. A* **75**, 063404 (2007).
- [40] X. Deng, S. Ray, S. Sinha, G. V. Shlyapnikov, and L. Santos, *Phys. Rev. Lett.* **123**, 025301 (2019).
- [41] G. L. Celardo, R. Kaiser, and F. Borgonovi, *Phys. Rev. B* **94**, 144206 (2016).
- [42] N. C. Chávez, F. Mattiotti, J. A. Méndez-Bermúdez, F. Borgonovi, and G. L. Celardo, *Phys. Rev. Lett.* **126**, 153201 (2021).
- [43] G. Dufour and G. Orso, *Phys. Rev. Lett.* **109**, 155306 (2012).
- [44] S. Flach, M. Ivanchenko, and R. Khomeriki, *Europhys. Lett.* **98**, 66002 (2012).
- [45] L. A. Toikka, *Phys. Rev. B* **101**, 064202 (2020).
- [46] D. Thongjaomayum, S. Flach, and A. Andreanov, *Phys. Rev. B* **101**, 174201 (2020).
- [47] S. Hermes, T. J. G. Apollaro, S. Paganelli, and T. Macrì, *Phys. Rev. A* **101**, 053607 (2020).
- [48] P. Jurcevic, B. P. Lanyon, P. Hauke, C. Hempel, P. Zoller, R. Blatt, and C. F. Roos, *Nature (London)* **511**, 202 (2014).
- [49] P. Richerme, Z.-X. Gong, A. Lee, C. Senko, J. Smith, M. Foss-Feig, S. Michalakis, A. V. Gorshkov, and C. Monroe, *Nature (London)* **511**, 198 (2014).
- [50] A. Safavi-Naini, M. L. Wall, O. L. Acevedo, A. M. Rey, and R. M. Nandkishore, *Phys. Rev. A* **99**, 033610 (2019).
- [51] T. Botzung, D. Vodola, P. Naldesi, M. Müller, E. Ercolessi, and G. Pupillo, *Phys. Rev. B* **100**, 155136 (2019).
- [52] X. Deng, G. Masella, G. Pupillo, and L. Santos, *Phys. Rev. Lett.* **125**, 010401 (2020).
- [53] B. Kloss and Y. Bar Lev, *Phys. Rev. B* **102**, 060201(R) (2020).
- [54] D.-M. Storch, M. van den Worm, and M. Kastner, *New J. Phys.* **17**, 063021 (2015).
- [55] V. Romero-Rochín, R. P. Duarte-Zamorano, S. Nilsen-Hofseth, and R. G. Barrera, *Phys. Rev. E* **63**, 027601 (2001).
- [56] K. Winkler, G. Thalhammer, F. Lang, R. Grimm, J. Hecker Denschlag, A. J. Daley, A. Kantian, H. P. Büchler, and P. Zoller, *Nature (London)* **441**, 853 (2006).
- [57] S. Mondal, A. Kshetrimayum, and T. Mishra, *Phys. Rev. A* **102**, 023312 (2020).
- [58] W. Li, A. Dhar, X. Deng, K. Kasamatsu, L. Barbiero, and L. Santos, *Phys. Rev. Lett.* **124**, 010404 (2020).
- [59] D. Petrosyan, B. Schmidt, J. R. Anglin, and M. Fleischhauer, *Phys. Rev. A* **76**, 033606 (2007).
- [60] M. Valiente and D. Petrosyan, *J. Phys. B: At., Mol. Opt. Phys.* **41**, 161002 (2008).
- [61] F. Stellin and G. Orso, *Phys. Rev. Res.* **2**, 033501 (2020).
- [62] S. Sarkar and T. Sowiński, *Phys. Rev. A* **102**, 043326 (2020).
- [63] V. E. Kravtsov, O. M. Yevtushenko, P. Snajberk, and E. Cuevas, *Phys. Rev. E* **86**, 021136 (2012).
- [64] E. J. Torres-Herrera, A. M. García-García, and L. F. Santos, *Phys. Rev. B* **97**, 060303(R) (2018).
- [65] R. Ketzmerick, G. Petschel, and T. Geisel, *Phys. Rev. Lett.* **69**, 695 (1992).
- [66] E. J. Torres-Herrera and L. F. Santos, *Ann. Phys. (Berlin, Ger.)* **529**, 1600284 (2017).
- [67] E. J. Torres-Herrera and L. F. Santos, *Phys. Rev. B* **92**, 014208 (2015).